Status of a Multiplexed Single Photon On-Demand Source

A. L. Migdall[a], S. Castelletto[a,b] and M. Ware[a]

[a]Optical Technology Division,
National Institute of Standards and Technology,Gaithersburg, Maryland 20899-8441
[b]Istituto Elettrotecnico Nazionale G. Ferraris, Turin Italy

ABSTRACT

We present the status of our work implementing a single photon on-demand source based on a multiplexed arrangement of parametric downconverters. An array of downconverters with multiplexed outputs makes it possible to create light pulses with increased probability of containing a single photon, while suppressing the probability of producing more than one photon. This is crucial for quantum cryptographic applications. Our current setup implements the scheme in a greatly simplified manner that produces photons along with a measure of the likelihood that the light pulse emitted is just a single photon. This implementation uses a virtual array of downconverters and an array of staggered length optical fibers allowing a single detector to measure a herald photon output by a series of downconverters. This single detector arrangement is a great savings considering the cost of such detectors. The timing of the herald tells us which path the herald took, which in turn, provides information on the single vs. multiphoton probabilities. So far, our work shows that the individual correlated photon peaks are clearly resolvable with our 2.4 ns delay line steps and the 1 ns full width half maximum (FWHM) of the correlated photon peaks, and that we can observe four correlated photon peaks simultaneously, a requirement to fully implement our scheme. Our current efforts are to increase the brightness and utility of the system for incorporation into a quantum communication testbed.

Keywords: single photon, quantum cryptography, parametric downconversion, heralded photon

1. INTRODUCTION

The emerging applications of quantum computation and quantum communication[1–10] have increased the need for light sources that produce individual photons. While a number of newer schemes relying on individual quantum systems are being developed as single photon sources,[11–14] most implementations to date have relied on either faint lasers or low rate parametric down conversion (PDC) setups.[9,15–18] Each of these traditional schemes suffers from the drawback that they cannot be made to exclusively emit single photons at a high rate. This is because these sources emit photons with statistical distributions (Bose-Einstein, Poisson, or a combination of both), so there is no way to make the single photon emission rate approach unity. More specifically, the probability of emitting two photons depends roughly on the square of the single photon rate. Thus the need to minimize the likelihood of producing multiple photons forces these sources to be operated at low rates of single photon emission.

In previous work[19,20] we proposed and analyzed a scheme that deals with this problem by using a multiplexed array of PDC sources. The scheme allows the emission of single photons at a higher rate, while suppressing the multiphoton rate. We also presented a simplified version of that scheme, that greatly eases the physical implementation, while still retaining significant advantage over the usual single PDC and faint laser source schemes. We have constructed a four-channel implementation of this simplified scheme and present the status of that work.

We begin with a brief summary of the original fully multiplexed scheme along with the simplified version that we have implemented. For complete details see our previous work.[19,20] The full system is shown conceptually as an array of downconverters and detectors in Fig. 1. All of the downconverters are pumped simultaneously

Further author information: (Send correspondence to A. L. Migdall)
A. L. Migdall: E-mail: amigdall@nist.gov, Telephone: 1 301 975 2331, FAX: 1 301 869 5700
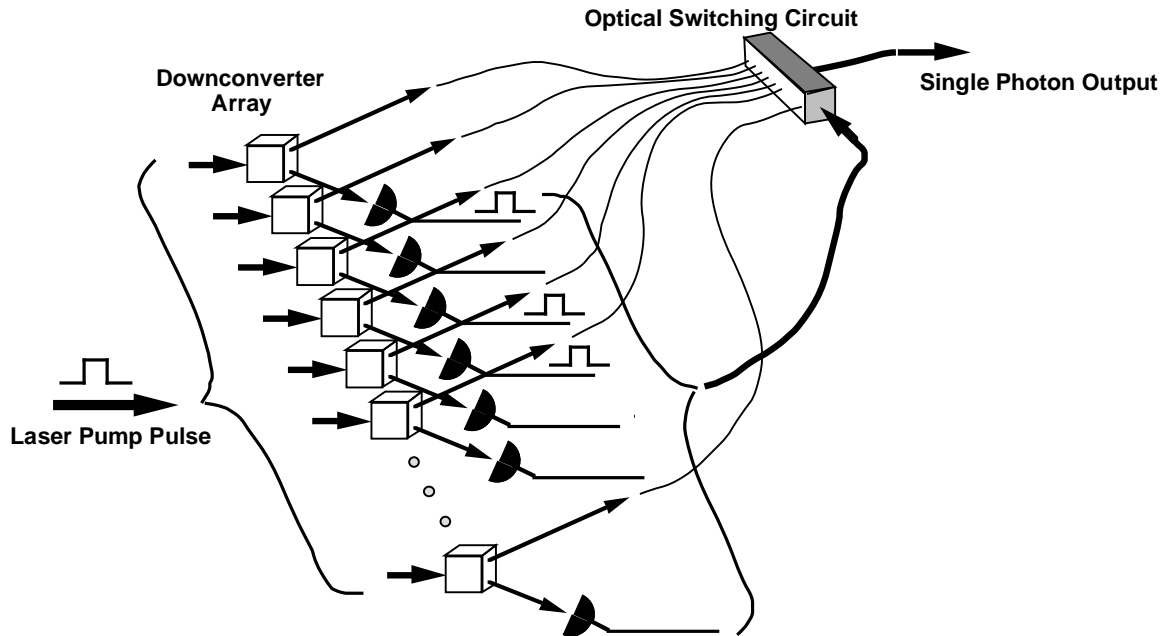
Figure 1. General schematic for single photon source showing array of crystal downconverters each with the potential of producing a pair or pairs of photons. Each downconverter is shown with its own trigger detector. The information about which trigger detectors have fired is sent to the optical switching circuit to control which incoming lines are directed to the output line. Input line delays to allow the trigger information to arrive before the incoming photons are not shown.

by the same laser pulse. The pump laser power is chosen so each downconverter has some small probability of producing a photon pair, while the number of downconverters is chosen so there is a high likelihood of at least one photon pair being created somewhere in the array. The detector associated with each downconverter indicates which of the downconverters has fired. This information is used to control an optical switching circuit directing the other photon of the pair into the single output channel. This arrangement allows higher single photon rates while maintaining low multiphoton emission rates – a much truer approximation of a single photon on-demand source than is possible without multiplexing.

Our initial implementation of this scheme involves three simplifications (Fig. 2) that allow us to test some of aspects of the complete scheme, while still producing a single photon source that yields significant advantages over the traditional single channel PDC source. The first simplification (Fig. 2a) is to implement the array of PDC sources with a single crystal. Because we use Type I phasematching, the PDC light is emitted with azimuthal symmetry around the pump beam. Thus we can arrange trigger detectors and the collection paths correlated to those trigger directions at different azimuthal angles around the pump beam.

The second simplification (Fig. 2b) allows the array of detectors to be replaced by a series of staggered length optical fibers and a single detector. Each of the trigger photons is coupled into an optical fiber of a unique length. The output ends of the fibers are all bundled together and sent to the single detector. Now, the timing of the firing of the trigger detector relative to the pump pulse tells us which one of the output paths contains a photon.

The final simplification (Fig. 2c) replaces the optical switching circuit with a single collection lens. This significantly changes the operation of the system, but it still retains certain advantages over the conventional single channel systems. This simplified system now produces light pulses along with one additional bit of information - i.e. which trigger path contained the photon correlated to the output photon. As shown in our previously published calculations,[19, 20] that piece of information can be directly mapped onto the single-photon probability. Thus each output pulse from the system comes with an individualized single photon "certification." This certification is the likelihood that the emitted pulse is just a single photon. These individualized certifications
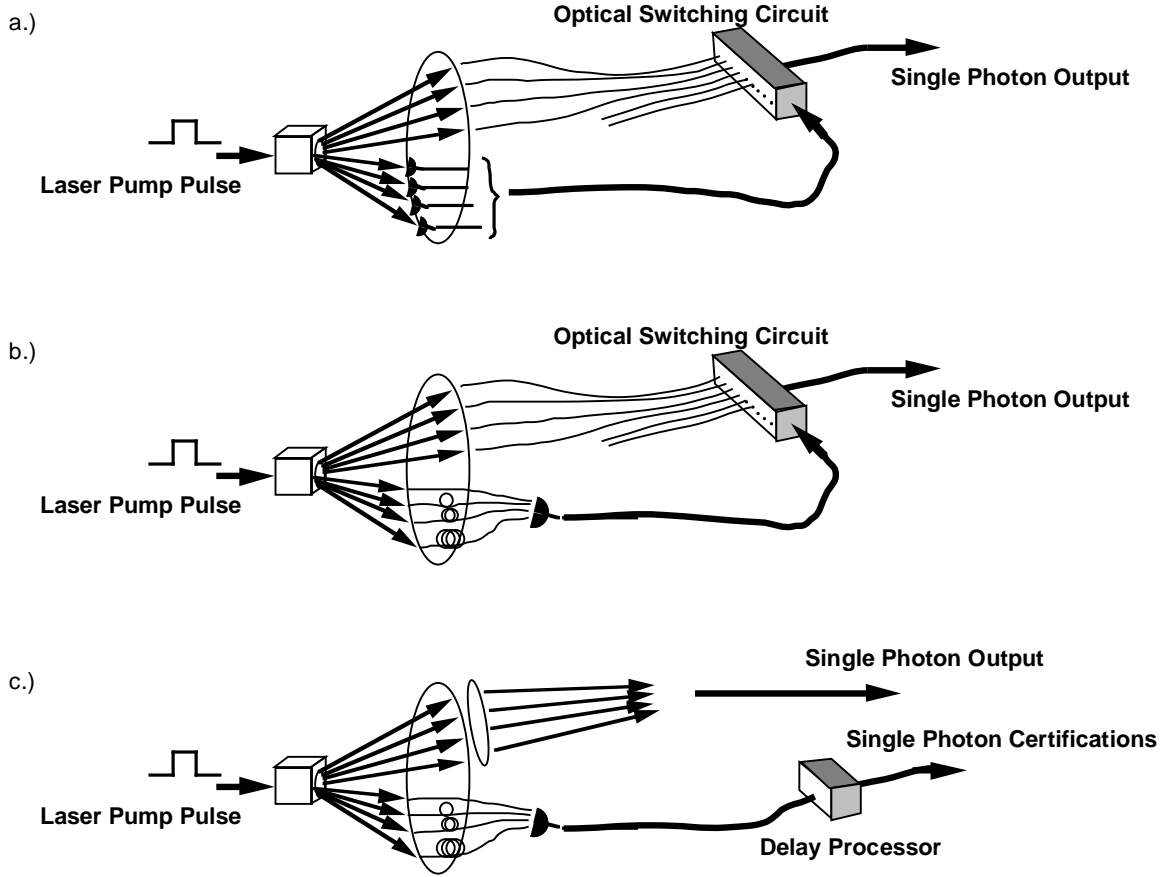
Figure 2. a.) Single crystal implementation of scheme. b.) Single detector implementation of scheme. Sequential series of delay lines is seen leading to the trigger detector. c.) Implementation without the optical switching circuit. A lens is used to collect all the modes correlated to those seen by the trigger.

allow more efficient use of single photon resources in a quantum encrypted communication system relative to such overhead tasks as privacy amplification.

The results of our previous analysis of this last scheme showed that for a Bose-Einstein distribution, the resulting single photon certifications for a system of N_{D} trigger delay paths are given by:

$$P_{\overline{n},\eta,N_{\mathrm{D}}}(i) = \left(\frac{N_{\mathrm{D}}}{\overline{n} + N_{\mathrm{D}}} \right)^{i-1+N_{\mathrm{D}}} \times \left(\frac{N_{\mathrm{D}} + \eta\overline{n}}{\overline{n} + N_{\mathrm{D}}} \right)^{i}, \tag{1}$$

where $\overline{n}$ is the mean photon number of the entire PDC array per pulse and η is the trigger detector detection efficiency. Fig. 3 shows the calculated certifications for a range of $\overline{n}$ and η. Curves indicating the single photon probability of faint laser and single PDC sources are shown for comparison. Because the advantage of this PDC array source is most evident in the region of the upper right of the matrix of Fig. 3, i.e., high η and $\overline{n}$ above 0.5, it is our goal to move our prototype into this region of operation.

2. EXPERIMENT

Our experimental setup (Fig. 4) consists of an Ar^{+} laser operating at a wavelength of 458 nm and mode locked at a 82 MHz repetition rate. An electro-optic light modulator is used to reduce pump pulse rates if necessary. The beam pumps a KDP ($\mathrm{KH_2PO_4}$) crystal at near normal orientation. The cut of the crystal ($43°$) is such that output light at the degenerate wavelength of 916 nm is emitted at $\approx 2.75°$ away from the pump beam direction.
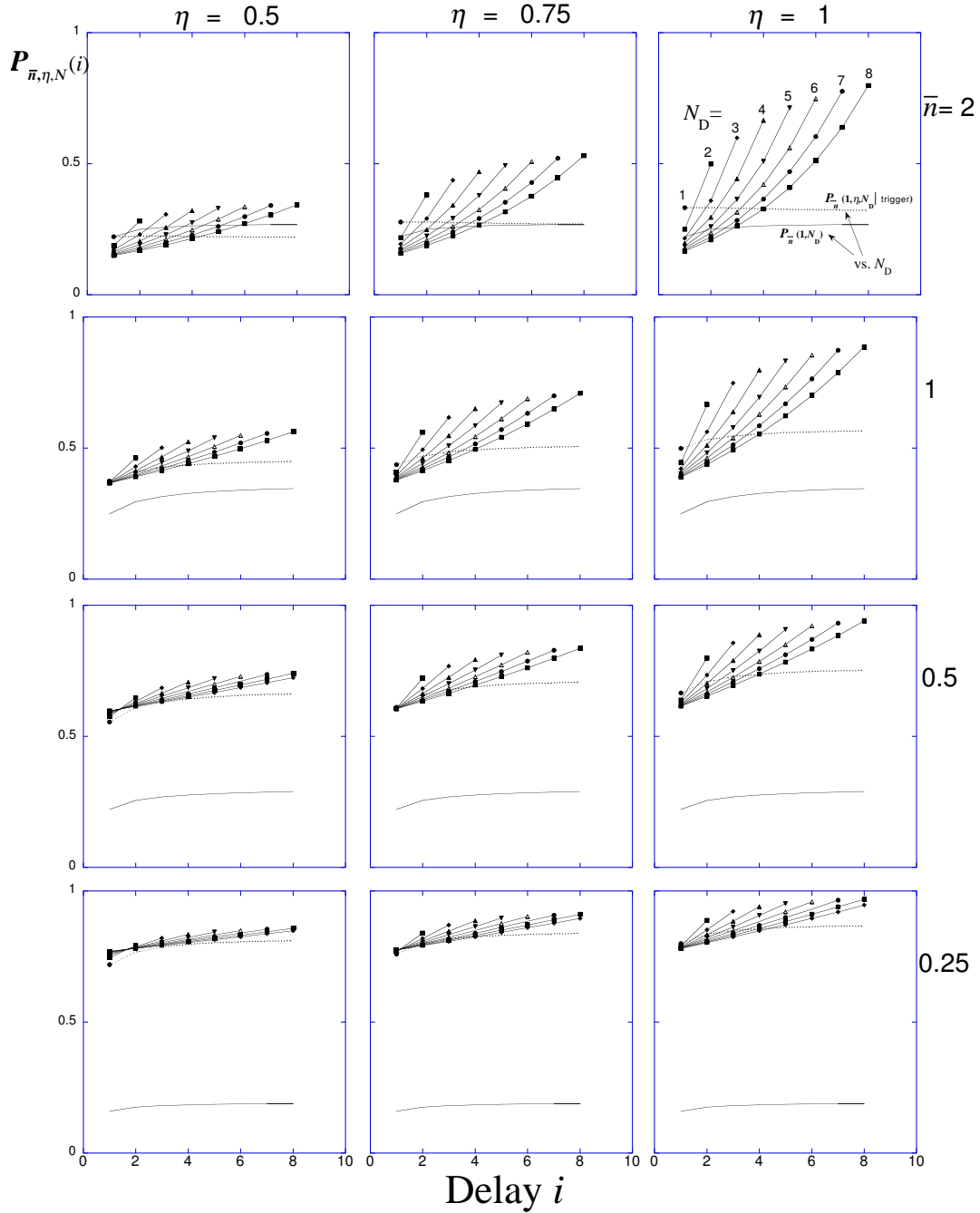
Figure 3. Matrix of graphs of single photon "certifications," $P_{\overline{n},\eta,N_{\mathrm{D}}}(i)$ as a function of the ith delay firing for a range of values of $\overline{n}$ and η. The columns correspond to η's of 0.5, 0.75, and 1 from left to right, while the rows correspond to $\overline{n}$'s of 2, 1, 0.5, 0.25 from top to bottom. For example in the upper right graph, the fan of curves labeled 1-8 are the probabilities of exactly one photon being produced given that the ith delay, in a system of N_{D}, caused the trigger to fire for $\eta=1$ and $\overline{n}=2$. The lowest curve in each graph is the total probability for a system of N_{D} delays to produce a single photon per pump pulse. The dashed curve is that same probability that the emitted light is a single photon given that the trigger did fire. (For these last 2 curves, the x-axis is N_{D} rather than triggered delay.)
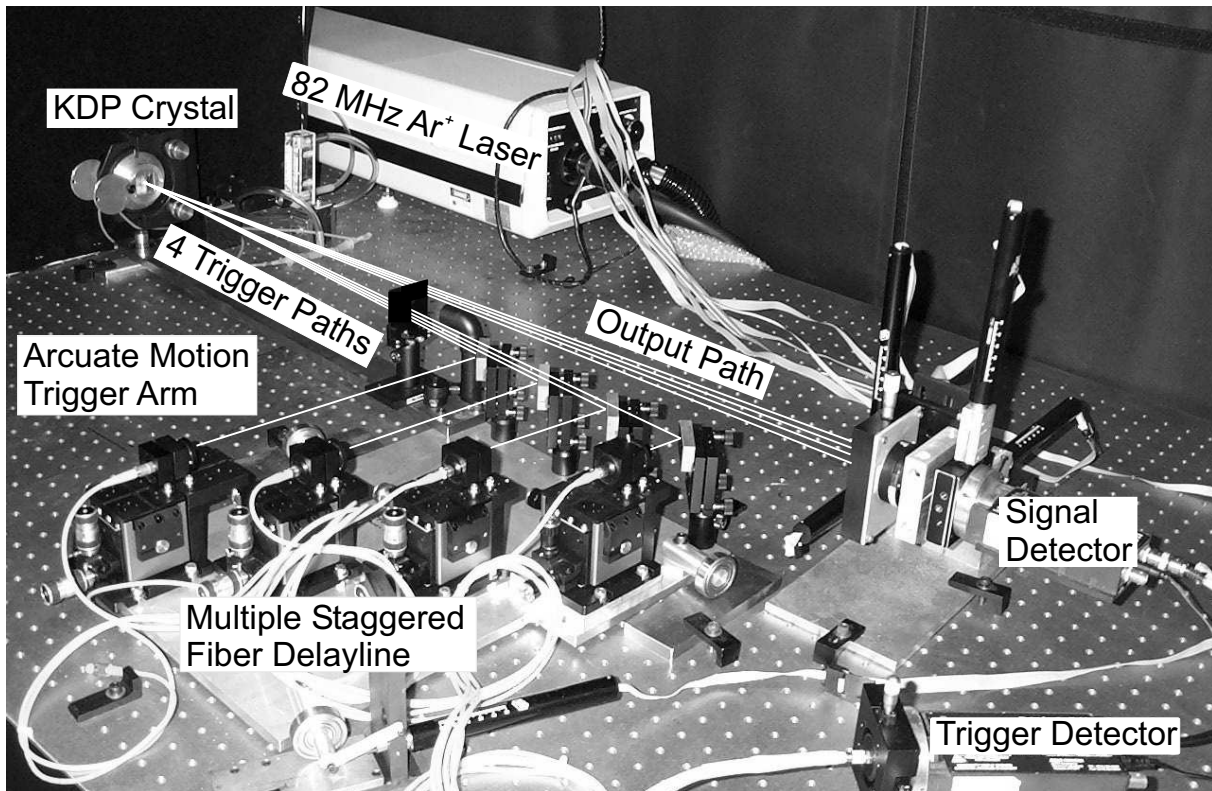
Figure 4. Photo showing setup and beam paths.

Short wavelength absorbing glass filters are used in the trigger and signal beam paths to block scattered light at the pump wavelength. We collect four trigger channels with mirrors staggered in height to pick off four adjacent beam paths. The mirrors are positioned so that each subsequent beam passes as close as possible to the previous mirror without being clipped by it. The mirrors direct each beam to a 5.7 mm aperture aspheric lens that couples the light into a 5.5 μm core single mode fiber. (The single-mode of each fiber defines the single spatial modes collected.) The four fibers and collection lenses are held by high precision 3 axis flexure stages. To ease system alignment, these four flexure stages are mounted on a single plate that rotates about an axis through the PDC crystal, providing arcuate motion. Thus, once the fibers and lenses are aligned, the collection angle of the PDC light can be varied while the collection modes stay overlapped with the crystal region pumped by the laser. This allows the collected wavelength of the PDC light of all four channels to be adjusted simultaneously. The distance from the crystal to the fiber collection lenses is 1 m for all four paths. The fiber output ends are stripped to their cladding (125 μm), bundled together, and imaged onto a single detector, a Si APD (avalanche photodiode) using reducing optics to assure that the 0.2 mm diameter detector area is underfilled. The fiber bundle consists of 6 fibers of increasing lengths with 0.5 m differences, corresponding to 2.4 nm optical delay differences. While only four fibers are needed for this setup, having six fibers allows for some variability of the delay spacing between fibers and possible fiber breakage.

The PDC signal beam light correlated to the light collected by the trigger fibers is collected by a single lens and imaged directly onto a Si APD. The crystal-to-signal lens distance is the same as for the trigger channels, 1 m. The signal lens is apertured by a 1 mm by 25 mm slit oriented with the long axis along the tangent of the PDC light cone. The trigger and signal APD outputs are sent to the start and stop inputs, respectively, of a coincidence circuit.

3. RESULTS AND CONCLUSIONS

We include two data sets here to illustrate the operation of this setup: one taken with three of the four trigger channels blocked and one with light collected in all four channels. The resulting histograms of start-stop times are shown in Fig. 5. The upper curve shows the single channel data. The first peak is due to detection of trigger and signal photons produced by the same pump pulse. The subsequent peaks are accidentals due to a start from one pump pulse and a stop produced by a later pump pulse. The peak spacing of 12.2 ns corresponds to the repetition rate of the pump laser. These smaller peaks, which are not due to correlated photons from a single pair, are the effective background that must be subtracted from the first peak. Note that all of these background events are due to PDC light, but they are not due to a start and stop from the same photon pair. The size of this background depends on the total amount of PDC light collected by the signal detector. From the absolute count rates for the data set shown, the probability of detecting the photon correlated to the one seen by the trigger is about 4 % (i.e., this is the overall detection efficiency of the signal path). Also note that an aperture, installed in the signal beam to reduce the count rate at the detector to a safe level was in part responsible for this low detection efficiency. The likelihood that the signal channel sees a photon for any given pump pulse is 1 % (regardless of whether a trigger photon is detected). These two values are consistent with the relative sizes of the peaks in the upper curve. This background becomes more of a problem as the signal detector collects more PDC light that is not specifically correlated to the light seen by the trigger channel. We return to this problem shortly.
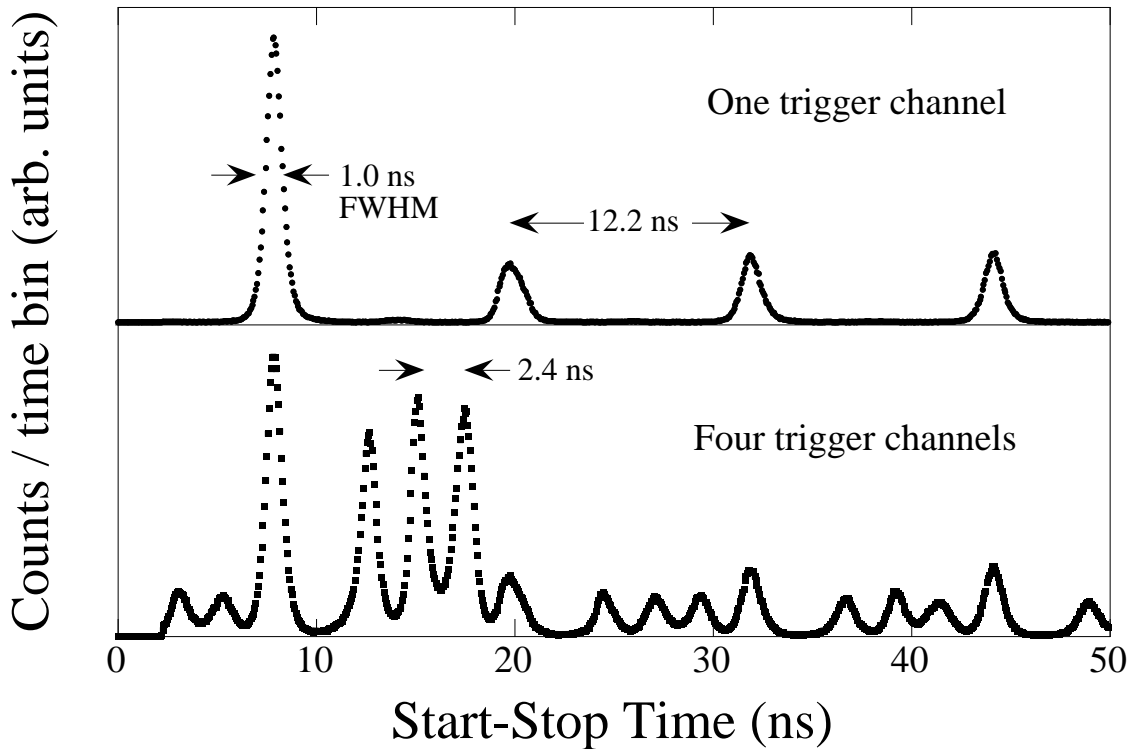
Figure 5. Histograms of start-stop intervals between trigger and signal detection events. The upper curve was taken only a single trigger channel open. The lower curve was taken with 4 trigger channels.

The lower curve in Fig. 5 shows the result with all four trigger channels open. Now we see four large peaks each followed by their own associated uncorrelated background peaks spaced at multiples of 12.2 ns. The 2.4 ns time difference between fiber is clearly seen. For this setup an intermediate length fiber was skipped between the first and second trigger channel causing the double wide gap between the first and second peaks. The 1.0 ns FWHM peaks are easily resolvable with this 2.4 ns spacing, demonstrating that this arrangement will work with
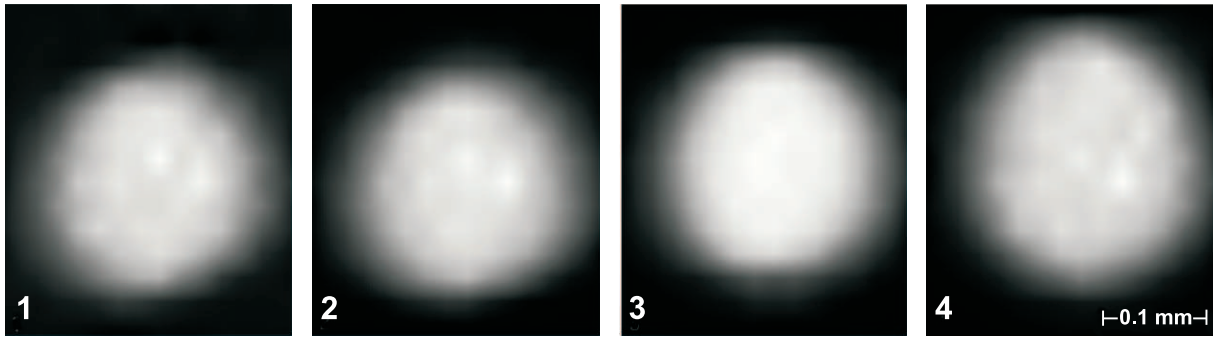
Figure 6. Maps of four coincidence channels made simultaneously by scanning the signal detector across the beams. Relative signal intensity is shown on a linear scale with white representing maximum intensity.

the existing electronics system.

As further demonstration of the system, we illustrate how we were able to use this resolvability of the different channels to align the signal lens-detector distance in the signal channel, which is important for efficient light collection and detection. When that distance is properly set, the four signal beams are focused to a single point by the lens. Transverse position scans of the signal detector (with focusing lens fixed) were made by setting time windows around each of the four histogram peaks (lower curve of Fig. 5) and simultaneously recording the coincidence counts of the four channels. For each peak the corresponding background peak was subtracted out. The resulting four maps of coincidence counts are shown in Fig. 6. The detector active area diameter is about 0.2 mm, as can be seen by the spot size. The sharpness of the edges indicates that the spot size is 50 μm or less, thus we can be assured that all the light entering the lens lands within the detector active area. Any misfocusing of the signal lens is seen as relative shifts of the four peaks, as well as reduced edge sharpness. Figure 7 shows the shift of two of the four channels as the detector-lens distance is varied in 0.6 mm steps, demonstrating the sensitivity of the method. Fig. 6 was made after focusing the signal lens using this alignment procedure. Here the residual shifts of the spots were less than 20 μm, indicating the detector was within 65 μm of the focus of the 50 mm focal length collection lens.
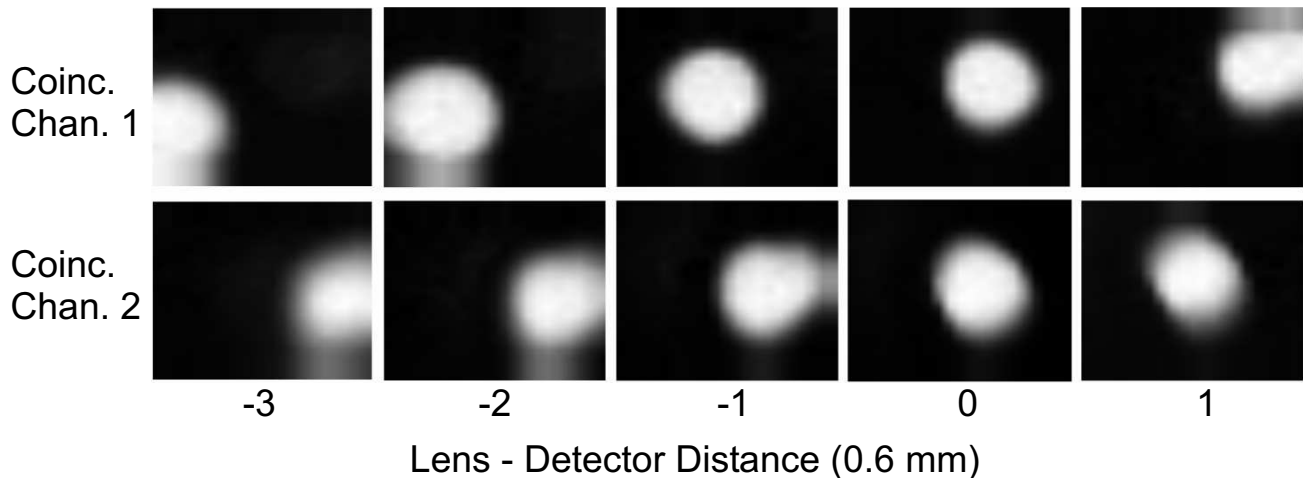
Figure 7. Maps of two coincidence channels taken as the collection lens detector distance was varied in 0.6 mm steps.

From the data presented here, it is clear that it will be necessary to restrict the excess light collected by the signal channel, i.e. light uncorrelated to the trigger spatial modes. This is due to the limited dynamic range of the signal detector. In theory we could collect all the light correlated to the four trigger beams, along with all

the light in between and a significant amount surrounding the beams. Unfortunately, in practice this will swamp the signal detector, because in general it can only handle at most a few million cts/s. For the above data sets we ran with trigger count rates of $\approx 14\mathrm{x}10^3$ cts/s/chan, while the signal channel had a rate of $\approx 10^6$/s, close to the maximum limit. Note that the narrow signal slit width of 1 mm, that was needed to reduce the signal rate to the 10^6/s level, also significantly reduced the collection of the light correlated to the detected trigger photons. This is a limitation imposed more by the detector rather than by the method itself, as the correlation and time resolution would allow a GHz count rate limit, not the current few MHz rate.

Our current plans for this system include increasing the efficiency of the PDC production, increasing the detection efficiency, and reducing the uncorrelated light seen by the signal detector. These improvements are needed to move the operation of the multiplexed source toward the most advantageous region of the $\overline{n}$ and η map shown in Fig. 3, i.e., higher $\overline{n}$ and η. The PDC efficiency will be increased by using $KNbO_3$ with nonlinear coefficient d_{eff} 37 times greater than that of KDP, yielding a 1344 times higher conversion efficiency. This should produce $\overline{n}$'s > 0.5, up from the current value of less than 0.001. We plan on reducing the uncorrelated light collected by replacing the single lens in the signal beam paths with a four channel fiber collection setup similar to the trigger collection setup. This will allow us to better characterize the existing certified single photon source, as well as prepare the way for the full multiplexed version that requires individual collection fibers for the signal paths anyway. This reduction of unwanted light will also allow us to improve collection efficiencies somewhat, although additional improvement will be needed. We are exploring a switch to other wavelengths where our detectors have higher η, as well as switching to other more efficient detectors to achieve the needed overall collection efficiency. Each of these improvements will move us toward our goal of creating a practical source of single photons for cryptographic applications.

REFERENCES

1. C. Bennett and G. Brassard, "Quantum cryptography: public key distribution and coin tossing," in *Proceedings of the IEEE International Conference on Computers, Systems and Signal Processing*, p. 175, 1984.

2. C. Bennett and G. Brassard, "Quantum public key distribution system," *IBM Technical Disclosure Bulletin* **28**, p. 3153, 1985.

3. C. Bennett and G. Brassard, "The dawn of a new era for quantum cryptography: The experimental prototype is working!," *SIGACT NEWS* **20**, p. 78, 1989.

4. C. H. Bennett, F. Bessette, G. Brassard, L. Salvail, and J. Smolin, "Experimental quantum cryptography," *Lecture Notes in Computer Science* **473**, pp. 253–265, 1991.

5. A. Ekert, "Quantum cryptography based on bell's theorem," *Phys. Rev. Lett.* **67**, pp. 661–663, 1991.

6. C. Bennett, "Quantum cryptography using any two nonorthogonal states," *Phys. Rev. Lett.* **68**, pp. 3121–3124, 1992.

7. C. H. Bennett, G. Brassard, and N. D. Mermin, "Quantum cryptography without bell theorem," *Physical Review Letters* **68**(5), pp. 557–559, 1992.

8. A. K. Ekert, J. G. Rarity, P. R. Tapster, and G. M. Palma, "Practical quantum cryptography based on 2-photon interferometry," *Physical Review Letters* **69**(9), pp. 1293–1295, 1992.

9. W. Tittel, J. Brendel, H. Zbinden, and N. Gisin, "Quantum cryptography using entangled photons in energy-time bell states," *Physical Review Letters* **84**(20), pp. 4737–4740, 2000.

10. E. Knill, R. Laflamme, and G. J. Milburn, "A scheme for efficient quantum computation with linear optics," *Nature* **409**, pp. 46–52, 2001.

11. J. Kim, O. Benson, H. Kan, and Y. Yamamoto, "A single-photon turnstile device," *Nature* **397**, pp. 500–503, 1999.

12. M. M. P. J. C. G. F. S. P. Michler, A. Imamoglu and S. K. Buratto, "Quantum correlations among photons from a single quantum dot at room temperature," *Nature* **406**, pp. 968–970, 2000.

13. Z. Yaun, B. Kardynal, R. Stevenson, A. Shields, C. Lobo, K. Cooper, N. Beattie, D. Ritchie, and M. Pepper, "Electrically driven single photon source," *Science* **295**, pp. 102–105, 2002.

14. T. G. J. P. A. Beveratos, R. Brouri and P. Grangier, "Nonclassical radiation from diamond nanocrystals," *Phys. Rev. A* **64**, p. 061802, 2001.

15. B. C. Jacobs and J. D. Franson, "Quantum cryptography in free space," *Optics Letters* **21**(22), pp. 1854–1856, 1996.

16. W. T. Buttler, R. J. Hughes, S. K. Lamoreaux, G. L. Morgan, J. E. Nordholt, and C. G. Peterson, "Daylight quantum key distribution over 1.6 km," *Physical Review Letters* **84**(24), pp. 5652–5655, 2000.

17. T. Jennewein, C. Simon, G. Weihs, H. Weinfurter, and A. Zeilinger, "Quantum cryptography with entangled photons," *Physical Review Letters* **84**(20), pp. 4729–4732, 2000.

18. D. S. Naik, C. G. Peterson, A. G. White, A. J. Berglund, and P. G. Kwiat, "Entangled state quantum cryptography: Eavesdropping on the ekert protocol," *Physical Review Letters* **84**(20), pp. 4733–4736, 2000.

19. D. B. A. L. Migdall and S. Castelletto, "Tailoring single-photon and multiphoton probabilities of a single-photon on-demand source," *Phys. Rev. A* **66**, p. 053805, 2002.

20. S. C. A. L. Migdall, D. Branning and M. Ware, "Single photon source with individualized single photon certifications," *SPIE* **4821**, pp. 455–465, 2002.